Structures 3 (2015) 244–249

Contents lists available at ScienceDirect

Structures

journal homepage: http://www.elsevier.com/locate/structures

Torsional stiffness bounds of helical structures under the influence of kinematic constraints

Nikolaos Karathanasopoulos *

Institute for Mechanical Systems, ETH Zürich, Leonhardstrasse 21, CH-8092 Zürich, Switzerland

ARTICLE INFO

Article history:
Received 15 December 2014
Received in revised form 16 May 2015
Accepted 18 May 2015
Available online 28 May 2015

Keywords:
Helix
Kinematics
Torsion
Constraint

ABSTRACT

The current work provides a framework for the assessment of the mechanical response bounds of multilayer helical assemblies. To that extent, the effect of structural kinematic constraints is analyzed, considering a wide range of braiding patterns for the helical assembly. Thereupon, torsional response bounds are retrieved, introducing scaling factors that relate the stiffness properties of the kinematically constrained structure to analytical, closed-form expressions.

1. Introduction

Helical structures are encountered in various forms of layered assemblies, such as ropes, cables [1] and electricity power transfer conductors [2]. Their structural response has been characterized with the use of both analytical and numerical models.

On the analytical modeling side, the helix axial and torsional loading response has been assessed by means of closed-form expressions, primarily derived upon thin beam theory considerations. In particular, Hruska provided analytical stiffness expressions that were solely based on the axial stiffness of the helix cross section [3]. McConnell et al. emphasized on the role of the helix cross-section torsional stiffness [4], while closed-form expressions incorporating contributions of the axial, torsional and bending helix cross-section stiffness (*EA*, *GJ* and *EI* respectively) were provided by Sathikh et al. [5]. On the basis of the above contributing response mechanisms, a modeling advancement was presented, accounting for the radial loading structural response apart from the commonly considered axial and torsional ones [6]. Finally, experimental data on the static axial and torsional loading response ware provided for single and three layer helical assemblies [7,8].

On the numerical modeling side, Jiang et al. [9] elaborated a volume model based on the helical assembly structural symmetry, while a homogenization, beam element based model, applicable for beams with periodic micro-structures was presented by Cartraud et al. [10]. Limitations on the applicability of closed-form expressions were pointed out with the use of three dimensional finite element modeling [11]. Moreover, the effect of different inter-wire motions on the mechanical response of single layer helical assemblies was analyzed, concluding that it is the utter pivoting suppression that can have a substantial influence on the structural response and in particular on the torsional stiffness [12].

The mechanical behavior of multilayer helical assemblies was characterized by closed-form expressions formulated upon the response of the assemblies' single helical constituents [13]. Furthermore, the mechanical behavior of locked-coil geometries was addressed by means of analytically derived simplified routines. The latter were used to quantify the effect of the cross-section shape and size on the stiffness coefficients, concluding that any influence is rather minor for all practical applications [14]. Moreover, numerical models for the simulation of two layer [15] and three layer helical assemblies were presented [16] based on three dimensional finite element modeling.

Assessing the stiffness bounds of a helical assembly allows for the computation of the construction's loading bounds. The latter constitutes the basis for the analysis of its long term behavior. To that extent, Alani et al. studied the effect of mean axial loading on the endurance of helical strands [17], while the stress state that axial and bending loads induced was correlated to the fatigue life of ropes [18]. Furthermore, fretting damage phenomena were related to the axial and bending loading bounds to which the helical assembly was subject [19]. Finally, experimental studies highlighted the role of torsional loading as a failure mechanism of spiral ropes [20].

The weaving pattern of helical assemblies results in a discrete supporting of all helical layers, except for the innermost, as Fig. 1 schematically illustrates. Axially loading or externally anchoring the construction entails that the support positions – named as *trellis* points – are subject to compressive loads. The latter are either *self-induced* due to the radial forces that axial loading creates, or externally applied

* Tel.: +41 44 633 6331; fax: +41 44 632 1145.
E-mail address: nkaratha@ethz.ch.

http://dx.doi.org/10.1016/j.istruc.2015.05.004
2352-0124/

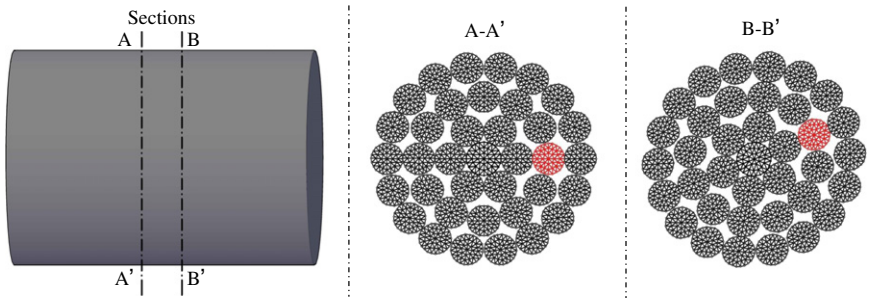

Fig. 1. Multilayer helical assembly support pattern.

(at the anchoring positions). As a result, the *trellis* points are contact boundaries that cannot be generally considered as load free, a conclusion experimentally verified upon post-failure inspection [21].

In the sections to follow, the torsional response of helical bodies positioned in multilayer helical assemblies is analyzed. More specifically, torsional stiffness bounds are derived considering the application of kinematic constraints at discrete positions along the helix development (Section 2). In particular, the effect of kinematic constraints applied at the helix cross-section normal rotational degree of freedom is assessed for different helical assembly structural arrangements. To that extent, scaling factors are introduced, quantifying the constraint effect with respect to analytical, closed-formed expressions (Section 3). A discussion on the obtained values along with concluding remarks follows in Section 4.

2. Model development

2.1. Helix geometry

The position vector **R**(s) of the helical body is defined as:

$$\mathbf{R}(s)=\begin{Bmatrix}R_x\\R_y\\R_z\end{Bmatrix}=\begin{Bmatrix}a\cos\varphi\\a\sin\varphi\\b\varphi\end{Bmatrix}\qquad \varphi=\frac{s}{\gamma}\qquad b=a\tan\theta \tag{1}$$

where a and b are intrinsic helix parameters. In particular, a stands for the distance at which the centerline position of the helix lies with respect to the origin and b for the along the helix central axis per unit angular evolution φ. Thereupon, the helix curvature κ and tortuosity τ are defined:

$$\kappa=\frac{a}{\gamma^2}\quad \tau=\frac{b}{\gamma^2}\quad \gamma=\sqrt{a^2+b^2}. \tag{2}$$

Fig. 2 depicts the afore-introduced geometric parameters along with the *Frenet-Serret* frame **n, b, t,** defined by means of the helix geometric parameters of Eqs. 1 and 2 as follows:

$$\mathbf{n}=\begin{bmatrix}-\cos\varphi\\-\sin\varphi\\0\end{bmatrix},\quad \mathbf{b}=\frac{1}{\gamma}\begin{bmatrix}b\sin\varphi\\-\cos\varphi\\a\end{bmatrix},\quad \mathbf{t}=\frac{1}{\gamma}\begin{bmatrix}-a\sin\varphi\\a\cos\varphi\\b\end{bmatrix}. \tag{3}$$

2.2. Helix closed-form structural response

The helix linear structural response upon an applied axial and torsional strain is described by a 2 × 2 stiffness matrix, relating the applied strains to a force and moment resultant along the *Cartesian* central axis *Z*:

$$\begin{bmatrix}F_z\\M_z\end{bmatrix}=\begin{bmatrix}\kappa_{\epsilon_z\epsilon_z} & \kappa_{\epsilon_z\omega'}\\ \kappa_{\omega'\epsilon_z} & \kappa_{\omega'\omega'}\end{bmatrix}\begin{bmatrix}\epsilon_z\\\omega'\end{bmatrix}. \tag{4}$$

Analytical models have provided closed-form expressions for the structural response as a function of different contributing mechanisms, namely of the axial *EA*, torsional *GJ* and bending *EI* helix cross-section stiffness (Section 1). Thereupon, the helix torsional stiffness $\kappa_{\omega'\omega'}$ has been analytically retrieved as [5]:

$$\kappa_{\omega'\omega'}=EAa^2c^2s+GJs^7+EIsc^2\left(1+s^2\right)^2\quad \kappa_{\omega'\omega'}(\theta\to 90^\circ)=GJ \tag{5}$$

where the abbreviations $s=\sin\theta$ and $c=\cos\theta$ have been employed. In the above expression *E* and *G* stand for the Young's modulus and for the shear modulus respectively, while *A* for the cross-sectional area and *I* and *J* for the helix cross-section central moments of inertia.

Eq. (5) predicts the torsional stiffness of a centrally torqued rod *GJ* for the geometric margin of a helix with a steep angle approaching $\theta\to 90^\circ$. The result reflects the equilibrium equations and the mechanical considerations upon which the stiffness expression has been derived. In particular, the internal forces and moments developed, solely follow the tangential (F_t, M_t) and binormal local vectors (F_b, M_b) as Fig. 2 illustrates, while no force or moment arises around the normal vector **n** of the helix cross-section.

2.3. Helix kinematic constraints

By applying a kinematic constraint on the normal rotational degree of freedom of the helix cross-section, a local moment M_n develops, as Fig. 3 schematically illustrates.

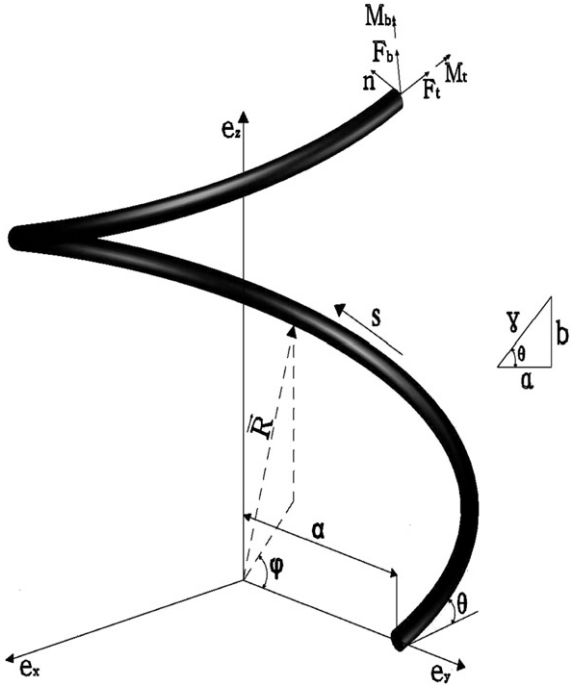

Fig. 2. Helix geometry.